

Chapter 8

Trace Gas Exchange at the Forest Floor

Matthias Sörgel, Michael Riederer, Andreas Held, Daniel Plake, Zhilin Zhu, Thomas Foken, and Franz X. Meixner

8.1 Introduction

The fluxes measured above an ecosystem are the net fluxes that integrate over all processes (see Chaps. 4 and 6). To quantify the different contributions from, for example, soil respiration and leaf gas exchange, they have to be measured separately, which classically has been achieved by applying enclosures. Recently, conditional sampling methods have also been applied to eddy-covariance (EC) measurements above canopy (Thomas et al. 2008; Zeeman et al. 2013, Chap. 6) to infer below canopy respiration fluxes. The study of Zeeman et al. (2013) utilizes the detection of coherent structures (Chap. 6) that are important drivers of the exchange throughout the canopy and can be used to qualitatively describe the coupling of the different layers of the forest (e.g., Thomas and Foken 2007). Normally, EC measurement systems have not been applied below 2 m (Thomas and Foken 2007; Serafimovich et al. 2011; Zeeman et al. 2013), and therefore decoupling of the forest floor from the layers above cannot be excluded. Furthermore, the influence of subcanopy advection (Chap. 6) on these measurements still needs to be clarified. Several studies

M. Sörgel (✉) • F.X. Meixner

Max Planck Institute for Chemistry, Biogeochemistry Department, Hahn-Meitner-Weg 1, 55128 Mainz, Germany
e-mail: m.soergel@mpic.de

M. Riederer

Ostbayerische Technische Hochschule Regensburg, Regensburg Center of Energy and Resources, 93049 Regensburg, Germany

A. Held

Atmospheric Chemistry, University of Bayreuth, 95440 Bayreuth, Germany

Bayreuth Center of Ecology and Environmental Research, University of Bayreuth, Bayreuth, Germany

(e.g., Baldocchi and Meyers 1991; Subke and Tenhunen 2004) successfully applied EC measurements below canopy to infer respiration fluxes. Application of data quality control for EC flux data (see Chap. 12) yielded a rejection rate of >60 % in the study of Subke and Tenhunen (2004), owing to the prerequisites of EC (like stationary conditions and well-developed turbulence) that are not always fulfilled below canopy. Furthermore, vegetation at the forest floor will influence respiration fluxes measured by EC (e.g., Misson et al. 2007). As they are cheap and relatively easy to handle, different designs of enclosures have been applied for decades to determine soil respiration fluxes, but without careful application, errors in fluxes can be large. Furthermore, chambers alter the natural layering above the surface and thus the diffusion gradient out of the soil, which alters the flux, although this effect has been reported to change the flux by less than 15 % (Davidson et al. 2002). The largest effect seems to be from altering pressure perturbations that are important for mass transport (e.g., Lund et al. 1999; Davidson et al. 2002) and from the exclusion of coherent structures and a longwave cooling (Riederer et al. 2014).

Another approach to the measurement of fluxes is the use of inert passive tracers like the radioactive noble gas radon. The decay of radioactive elements like uranium and thorium in soils leads to the exhalation of the radioactive noble gases such as ^{222}Rn and ^{220}Rn that have lifetimes of 3.5 days and 55.6 s, respectively. As radon is a noble gas, neither chemical reactions nor uptake by the biosphere change its concentration in air. Therefore, it is a perfect tracer for soil emissions. CO_2 , for example, is taken up by the understory vegetation and by the canopy when photosynthesis is active. Otherwise, the plants become a source as well due

D. Plake

UCL Umwelt Control Labor GmbH, Josef-Rethmann-Straße 5, 44536 Lünen, Germany

Z. Zhu

Key Laboratory of Ecosystem Network Observation and Modeling, Institute of Geographic Sciences and Natural Resources Research, Chinese Academy of Sciences, Beijing, 100101, China

T. Foken

Am Herrgottsbaum 28, 96120 Bischberg, Germany

Bayreuth Center of Ecology and Environmental Research, University of Bayreuth, Bayreuth, Germany

M. Riederer, T. Foken: Affiliation during the work at the Waldstein sites—University of Bayreuth, Department of Micrometeorology, Bayreuth, Germany

M. Sörgel: Affiliation during the work at the Waldstein sites—University of Bayreuth, Atmospheric Chemistry, 95440 Bayreuth, Germany

D. Plake, Z. Zhu: Affiliation during the work at the Waldstein sites—Max Planck Institute for Chemistry, Biogeochemistry Department, Hahn-Meitner-Weg 1, 55128 Mainz, Germany

to respiration at night. ^{222}Rn can be used to infer bulk diffusion coefficients by combining soil fluxes with profile measurements (Lehmann et al. 2001). A method for the direct determination of the transport time between two heights of a profile of ^{220}Rn has been proposed by Lehmann and coworkers (1999).

Alternatively, fluxes close to the surface can be calculated from profile measurements by using models. For the turbulent layer fluxes can be calculated in an iterative way from two heights according to the approach of Richter and Skeib (1984, 1991), henceforth named RS. As the transition from turbulent to laminar flow occurs close to the surface, there are also models available that explicitly calculate the fluxes for the different layers. These are referred to as hydrodynamic multilayer models (e.g., Foken 1979, 1984), as they were derived from hydrodynamic investigations.

In this chapter we present results from the EGER IOP 2 campaign (Chap. 1) at the Waldstein site, which examined the trace gas exchange at the forest floor. The central issue to be addressed is how coupling/decoupling of the near forest floor layer (below the height at which sonic anemometers can be applied) can be detected and the consequences of decoupling for flux measurements higher above (see Chap. 6). We use a multilayer model together with profiles with high vertical resolution close to the forest floor in order to compare modelled and measured surface concentrations of ^{222}Rn , CO_2 , H_2O , and O_3 . The model is first validated against sensible heat flux measurements by eddy covariance, and then calculated effective surface concentrations and measured surface concentrations of these different compounds (inert => very reactive) are compared. The influence of driving forces of trace gas exchange (radiation, turbulence, stability, and coupling) below canopy on the measurement of (reactive) trace gases profiles will be discussed.

8.2 Materials and Methods

8.2.1 Site Description

All investigations described in this chapter were done at the Waldstein-Weidenbrunnen site near the “Main Tower” (M1), which is described in detail in Chap. 2. The measurements were conducted during the intensive measuring period IOP 2 (June–July 2008) of the EGER project (Chap. 1). For the measurements near the ground, an additional, 2 m high, structure was installed at the forest floor. The forest floor measurements during IOP 2 were made around 25 m west-south-west of the main tower (see Fig. A1.2; Appendix A). Chamber measurements were also installed nearby. For further details see Appendix A.

8.2.1.1 Wind, Temperature, and Radiation Measurements

The wind profiles at the forest floor were measured by two-dimensional sonic anemometers (WS425, Vaisala, Helsinki, Finland) at 0.03 m, 0.30 m, 1.0 m, and 2.00 m above the ground. For measurements at the two lower heights, the anemometers were placed upside down and the wind direction was corrected afterwards. Temperature profiles were obtained by placing unshielded thermocouples (type E—chromel/constantan) at 0.01 m, 0.02 m, 0.04 m, 0.08 m, 0.3 m, 0.16 m, and 0.32 m and custom-built psychrometers (with active ventilation and radiation shielding) with thermocouples at 0.09 m, 0.26 m, 1.00 m, and 2.05 m.

Global radiation was measured by a pyranometer (type Li-200SZ, Licor, USA), net radiation by a net radiometer (type NR-lite, Kipp and Zonen, The Netherlands), and the photolysis frequency of NO_2 by a filter radiometer (Meteorologie Consult, Germany).

8.2.1.2 Trace Gas Measurements

Carbon dioxide soil flux was measured with a static chamber setup (Department of Environmental Geosciences, University of Basel, Basel, Switzerland; see Lehmann et al. 2004) and a commercial nondispersive infrared CO_2 analyzer (GMP343, Vaisala, Helsinki, Finland). ^{222}Rn fluxes were measured at the same chamber system by an alpha spectrometer (Alpha Guard, Genitron, Frankfurt, Germany). Soil fluxes of CO_2 and radon were derived from a linear rise of the trace gas concentration in the chamber during closure time according to Lehmann et al. (2004). The chamber had a diameter of 22.5 cm and the chamber system had a total volume of 10.2 L. The total volume consists of tubings, drying cartridges, 7.5 L chamber volume, and a 2.0 L delay volume to remove the ^{220}Rn . The chamber was closed every 3 h (IOP 1) or 2 h (IOP 2) for 50 min, which was long enough for a significant concentration rise and provided enough measurement points for radon (time resolution 10 min). Inside the chamber a ventilator mixed the enclosed volume. Additionally, profiles of ^{222}Rn and ^{220}Rn were measured at 0.00 m, 0.03 m, 0.1 m, and 0.3 m above ground. Two controlled valves were introduced to enable switching between two measurement heights measured by one analyzer. To improve the performance of the alpha guards, a Nafion drying system was introduced to dry the sample air. The sensitivity was 1 count per 20 Bq m^{-3} and the detection limit about 12 Bq m^{-3} . The alpha guards are not capable of distinguishing between the two measured radon isotopes. Therefore, the setup consists of two sets of two alpha guards. Each pair of analyzers had a delay volume of 0.0032 m^3 between the analyzer units. The flow through the system was kept constant to assure a mean residence time of the sample air in the delay volume of about 10 half-life times of ^{220}Rn , to solely (98 %) detect ^{222}Rn in the second instrument.

Reactive trace gases (NO , NO_2 , and O_3) and profiles of CO_2 and water vapor have been measured by a profile system by switching between inlets at different heights (close to the forest floor, 0.005 m, 0.03 m, 0.1 m, 0.3 m, and 0.9 m; within

the canopy, 3 m, 10 m, 16.5 m, and 20.5 m; as well as above canopy at 25 m and 31.5 m above ground level). We focus here on the measurement heights close to the forest floor (up to 1 m). The inlet tubes for the sample air were all 55 m long and protected by a Teflon filter (PTFE; pore size 5 μm), a funnel to prevent raindrops from entering and an insect-proof net at the inlet. The lines were isolated, heated, and radiation shielded. Furthermore, opaque Teflon tubes (blue pigments, 1/4") were used. The inlet for the lowest height was split into four inlets to reduce flow for each inlet from 7–9 L min^{-1} total to about 2 L min^{-1} for each inlet in order to reduce the effect of the local disturbance of the gradient by high airflows near the ground.

Nitrogen oxides (NO and NO₂) were measured by chemiluminescence analyzers (CLD 780 TR, Ecophysics, Dürnten, Switzerland). NO₂ was converted to NO by diode-based blue light converters (Droplet Measurement Technologies, Boulder, CO, USA). Ozone was measured by UV absorption (model 49c, Thermo Fischer Scientific, Franklin, MA, USA) and CO₂ and H₂O by nondispersive IR absorption (model 840, Licor, Lincoln, Nebraska, USA).

Ozone fluxes were measured by fast chemiluminescence O₃ sondes (GEFAS GmbH, Germany) and a Gill R2 3D ultrasonic anemometer (Gill, UK). The setup was placed at about 3 m distance from the forest floor station. Therefore, the O₃ signal of the fast instrument could not be used as an absolute signal and was only used for the fluctuations, with the mean signal being measured by a slow analyzer (in this case model 49c, see above). For more details regarding ozone fluxes see Chap. 9.

8.2.2 Modelling of Fluxes Near the Forest Floor

In contrast to the modelling approaches for the whole canopy (Chap. 16), simple parameterizations were used for the exchange at the forest floor. Instead of the simple bulk approach, which is usually applied to two fixed levels (surface and 10 m height), an approach with the profile coefficient Γ (Foken 2008) that integrates over the lowest layers was applied:

$$Q_H = \Gamma (T_1 - T_2) \quad (8.1)$$

Eq. (8.1) and the following equations were written for the sensible heat flux (in kinematic units), but they are similar for trace gas fluxes. This approach was used in two different ways:

1. The measuring heights z_1 and z_2 are in the upper part of the profile in the trunk space but at a distance that is large enough to measure a significant gradient. In contrast to simple two-point parameterizations, the applied method according to Richter and Skeib (1984, 1991), hereafter named RS, is also applicable in a stratified layer. From temperature and wind profile measurements, the calculation of the Obukhov length and of the Richardson numbers is possible.

2. For measuring heights $z_1 = 0$ and z_2 an aerodynamic approach according to Foken (1979, 1984) was applied. This approach is parameterized for the molecular or laminar layer (thickness 0.001 m), the molecular-turbulent buffer layer (thickness 0.01 m) and the neutral or stratified turbulent layer. As some of the parameterizations are derived from hydrodynamical arguments, the parameterization is called the hydrodynamic multilayer model (hereafter simply called multilayer model). It was applied to calculate the conditions at the surface for a given flux, for example, surface temperature for a given sensible heat flux. This calculated surface temperature is often not identical with the true surface temperature (Sodemann and Foken 2005; Lüers and Bareiss 2010), which indicates a decoupling near the surface, and therefore the turbulent conditions in the trunk space cannot be applied in the vicinity of the surface.

For the calculation of the effective surface concentrations, both methods have been combined. The RS approach was used to calculate fluxes from two heights in the turbulent layer and the multilayer model to calculate the effective surface concentration from this given flux and the profile. The congruence of these modelled effective surface concentrations with measured surface concentrations is used as a criterion to define coupled and decoupled situations of the near forest floor layer (<1 m). This coupling mechanism has to be distinguished from the coupling of the canopy to the above air layers by coherent structures (Thomas and Foken 2007; Chap. 6).

8.2.2.1 Parameterization According to Richter and Skeib (1984, 1991)

The RS parameterization is based on the calculation of critical height z_c , which is the height of the dynamical sublayer. For $z > z_c$ the atmosphere is stratified. In this approach the universal function by Skeib (1980) is applied. For the calculation of the friction velocity u_* and the $u(z)$ obtained from wind measurements at two levels follows:

$$u(z_2) - u(z_1) = \frac{u_*}{\kappa} \cdot \left\{ \begin{array}{ll} \ln\left(\frac{z_2}{z_1}\right) & z_1 < z_2 < z_c \\ \ln\left(\frac{z_c}{z_1}\right) + \frac{1}{n_u} \left[1 - \left(\frac{z_2}{z_c}\right)^{-n_u} \right] & z_1 \leq z_c \leq z_2 \\ \frac{1}{n_u} \left[\left(\frac{z_1}{z_c}\right)^{-n_u} - \left(\frac{z_2}{z_c}\right)^{-n_u} \right] & z_c < z_1 < z_2 \end{array} \right\} \quad (8.2)$$

The part in the curly brackets divided by the von-Kármán-constant κ is the reciprocal profile coefficient. The sensible heat flux can be calculated in an

analogous manner

$$T(z_2) - T(z_1) = \text{Pr}_T \frac{Q_H}{\kappa u_*} \left\{ \begin{array}{ll} \ln\left(\frac{z_2}{z_1}\right) & z_1 < z_2 < z_c \\ \ln\left(\frac{z_c}{z_1}\right) + \frac{1}{n_T} \left[1 - \left(\frac{z_2}{z_c}\right)^{-n_T} \right] & z_1 \leq z_c \leq z_2 \\ \frac{1}{n_T} \left[\left(\frac{z_1}{z_c}\right)^{-n_T} - \left(\frac{z_2}{z_c}\right)^{-n_T} \right] & z_c < z_1 < z_2 \end{array} \right\} \quad (8.3)$$

with the turbulent Prandtl number Pr_T . The solution of the model can be done in an iterative way. The necessary calculation of the critical height and coefficients n_u and n_T are given in the original literature or by Foken (2008).

8.2.2.2 Parameterization According to Foken (1979, 1984)

This approach uses an integration of the profile coefficient from the surface up to a level in the neutral or stratified turbulent layer

$$\Gamma = \left(\int_0^z \frac{dz}{K_T + \nu_{Tl} + \nu_T} \right)^{-1}, \quad (8.4)$$

where K_T is the turbulent diffusion coefficient, ν_{Tl} the molecular-turbulent diffusion coefficient in the buffer layer, and ν_T the molecular diffusion coefficient. The following setting of the parameters is based on experimental work over the ocean (Foken et al. 1978); for details see the original literature or Foken (2008):

$$\Gamma = \frac{\kappa \cdot u_*}{\kappa \cdot \text{Pr} \cdot \frac{\delta_T^+ u_*}{\nu} + \kappa \cdot \delta_T^+ + \ln \frac{u_* z}{30 \nu}} \quad (8.5)$$

Here Pr is the Prandtl number, $\delta_T^+ \approx 4$ the dimensionless temperature difference in the buffer layer, $\delta_T \approx 6$ the dimensionless thickness of the molecular layer, and ν the kinematic viscosity. In the case of a stratified atmosphere, a fourth summand that reflects the stability dependency must be included in the denominator.

8.3 Results and Discussion

8.3.1 Driving Forces of Subcanopy Exchange

8.3.1.1 Radiation

On average, about 10 % of the shortwave radiation is able to penetrate the canopy and reach the forest floor as observed from measurements about 10 m south of the

forest floor measurements (see Appendix A). Generally, the radiation distribution at the forest floor is very variable in space and time (Chap. 14) due to different PAI (Chap. 2) and changing solar zenith angle over the day. The amount of attenuated radiation at the Waldstein site changes over the course of the day between 5 % and 40 % due to the canopy structures (Sörgel et al. 2011). Generally, the radiation balance below canopy was found to be dominated by longwave radiation in contrast to daytime conditions above the forest canopy. The incoming and outgoing longwave radiation fluxes were both about 400 W m^{-2} . As incoming and outgoing radiations were more or less balanced, there was no net contribution to the energy exchange. The direct influence of the radiation to the exchange conditions seems to be limited to spots of direct radiation, the so-called sunflecks. Passing sunflecks cause changes in the temperature profile and—due to heating of the ground surface—to stability as well (see Fig. 8.1). During IOP 2 global radiation was therefore below 25 W m^{-2} during most of the day (before 8:00 and after 14:30). Maximum values of 350 W m^{-2} to 600 W m^{-2} were reached at 10:00, and a second maximum with about 70 W m^{-2} was reached at 13:00. Net radiation followed the global radiation closely except for the peak in the afternoon. A small negative peak in net radiation during that period might be explained by the heterogeneity as well. It seems that the sensor itself was in the shadow but the ground below was heated by sunlight and was therefore increasing the outgoing radiation. Even larger differences

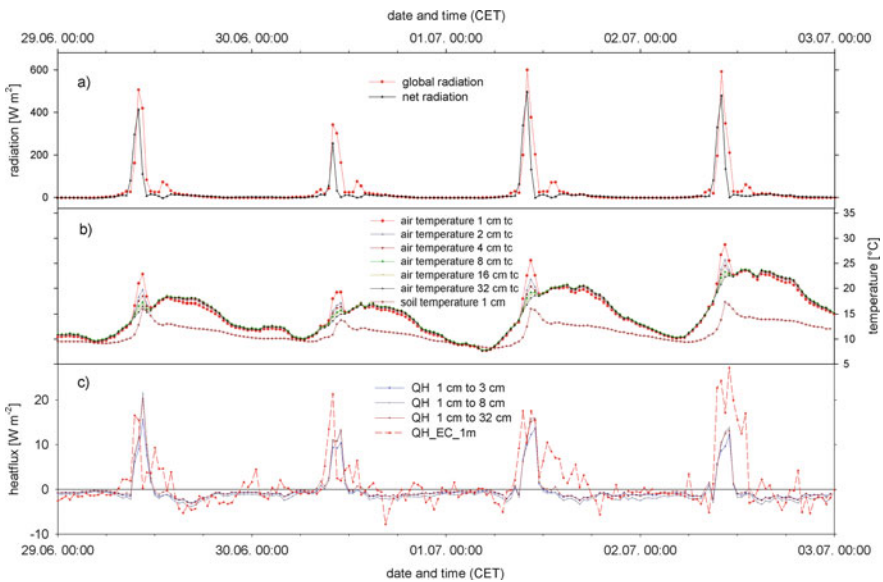


Fig. 8.1 Frame (a) shows global and net radiation measured at the forest floor site. A logarithmic profile of air temperature measured close to the ground surface with unshielded thermocouples and the soil temperature measured in 1 cm depth is shown in frame (b). Frame (c) shows sensible heat fluxes calculated from the temperature profiles by the multilayer model and for comparison the measured sensible heat flux from a nearby eddy covariance measurement at 1 m height

in magnitude and timing were found to radiation measurements of the four radiation components (longwave and shortwave in and out) at about 10 m horizontal distance (not shown here).

8.3.1.2 Temperature Profiles

During the golden days of IOP 2, the temperatures were between 7.7 °C and 28.7 °C at the forest floor (0.01 m) and between 7.6 °C and 23.7 °C at 1 m height. Temperature profiles showed consistently lowest temperatures at the forest floor, except for the time of day when sunflecks hit the ground below the sensors (Fig. 8.1). During those periods (8:00 to 12:00), positive temperature differences between 0.01 and 0.32 m of up to 7.5 K were observed. After those peaks the differences dropped to about zero and then became slowly negative, with the maximum negative values of about -1 K occurring in the evening (16:30 to 19:00). Thereafter, the temperature differences diminished, reaching values around zero in the early night.

8.3.1.3 Wind Profiles

Wind profiles in the lowermost 2 m show strong attenuation toward the ground and are log-linear between 1 m and 0.03 m except for very low wind speeds in the evening. Wind speeds at 2 m were higher than extrapolated from the profile between 0.03 and 1 m due to the more open trunk space in that height. Wind speeds at 2 m were on average 0.8 m s⁻¹ with maximum values of about 1.4 m s⁻¹. Wind speeds at 0.03 m hardly exceed 0.5 m s⁻¹ and are, on average, about 0.3 m s⁻¹. The average value for the same period at 1 m was 0.7 m s⁻¹, and the maxima were around 1 m s⁻¹. For comparison, the average wind speed above canopy at 32 m was 2.9 m s⁻¹ with a maximum of 4.7 m s⁻¹. Minima in wind speed at the forest floor occurred in the evening or in the early night during IOP 2. Coinciding with the minima in wind speed, wind direction changes (see Fig. 8.1). During daytime, winds at 1 m and 2 m were predominantly from the south, whereas at night the wind direction changed to east. A change in wind direction was consistently observed between the upper (1 m and 2 m) and the lower (0.03 m and 0.3 m) levels. This might be due to local channeling of the flow close to the ground. During daytime this difference was less obvious as wind speeds and wind direction were very variable.

8.3.2 Comparison of Measured and Modelled Fluxes

8.3.2.1 Friction Velocity

Wind speeds close to the forest floor were generally low due to the strong attenuation of the wind by the canopy although in the more open trunk space a secondary wind

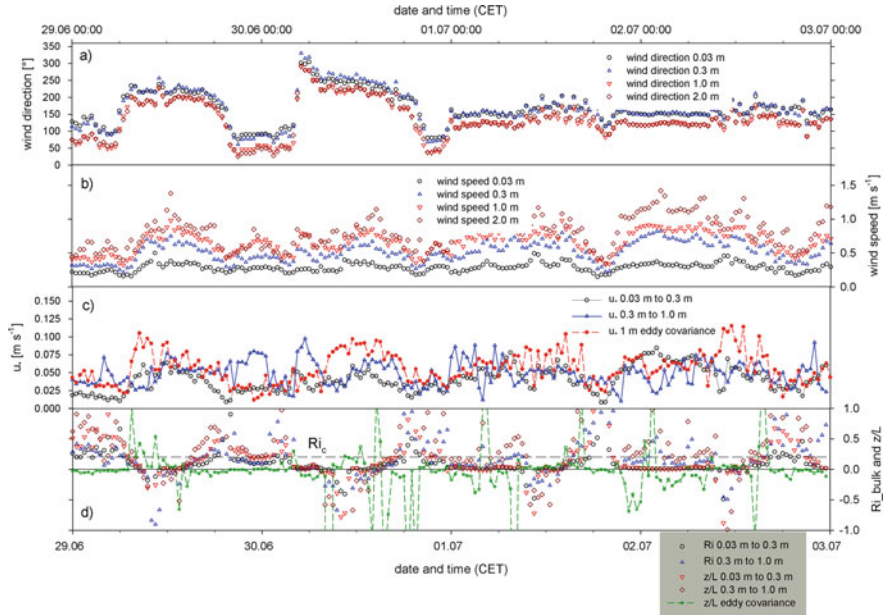


Fig. 8.2 Wind speed (frame **a**) and wind direction (frame **b**) in the lowest 2 m above the forest floor. Frame (**c**) shows the friction velocity calculated from the wind profile and for comparison the friction velocity determined by a nearby eddy covariance measurement. Additionally, the bulk Richardson number calculated from two different profile heights (0.03 m to 0.3 m and 0.3 m to 1 m) is shown in comparison to $\zeta = z/L$ determined from the same profile heights and as calculated from the eddy covariance measurements (frame **d**)

maximum occurs (see above). Nevertheless, close to the forest floor, the influence of the ground surface causes a strong attenuation as per definition the wind speed is zero at the surface. During IOP 2, wind speeds at 1 m height therefore hardly exceed 1 m s^{-1} . Consequently, values of the friction velocity are comparatively low as well. The diurnal cycle of u_* follows that of wind speed although due to higher scatter the diurnal course is less obvious (Fig. 8.2). Values are higher during daytime and lower during nighttime and show minima around sunset and in the early night coinciding with minima in wind speed and changes in wind direction. The u_* values derived from eddy covariance measurements, and those from the wind profiles agree within the variation, but differences can be up to a factor of two. Nevertheless, both methods show comparably small friction velocities (on average about 0.04 m s^{-1}) and therefore comparably (above-canopy average $u_* = 0.6 \text{ m s}^{-1}$) low turbulence. In addition to the locally produced turbulence from the shear of the horizontal wind, coherent structures that are generated above canopy play an important role in the exchange of canopy air with the above air layers (Thomas and Foken 2007; Serafimovich et al. 2011; Sörgel et al. 2011 and Chap. 6). These structures were found to occasionally reach down to 2 m (lowest measurement level), but it remains unknown if the mixing prevails down to the forest floor. From the results of Sörgel

et al. (2011), it was indicated that these structures provide mixing down to 0.5 m, as eddy covariance measurements are limited to some level above the forest floor and decoupling of the layers close to the surface can still occur below that measurement height.

8.3.2.2 Sensible Heat Flux

The multilayer model was developed for the determination of the energy exchange and was therefore compared to the sensible heat fluxes measured by eddy covariance at 1 m height. Sensible heat fluxes were calculated for several layers according to Eq. (8.1), with the profile parameters derived from the multilayer model according to Eq. (8.5). Temperature differences for the lower layers were derived from a profile (0.01 m to 0.32 m) of unshielded thermocouples. Although these temperature measurements might be influenced by radiation, there was no other available technique that could be used in the proximity of the surface. Furthermore, radiation was low for most of the day (see above). The shielded and actively ventilated thermocouples had a minimum installation height of about 0.1 m. Due to the active ventilation they also disturb the layering near the surface and thus the natural gradient. Therefore, they were just used for the upper part of the profile (0.1 m to 1 m). A shielding without active ventilation would result in a temperature measurement that is not equilibrated with the surrounding air due to the low wind speeds at the ground. Therefore, the unshielded thermocouples were used. Having these difficulties in mind, the agreement between the heat fluxes derived from the multilayer model and those from the eddy covariance is surprisingly good (see Fig. 8.1). At night all fluxes are nearly zero (detection limit of sensible heat flux $>5 \text{ W m}^{-2}$; e.g., Nordbo et al. 2012) except for short turbulent events or coherent structures that touch down into the trunk space (Chap. 11). Daytime fluxes coincide with direct radiation (see above) and reach up to 25 W m^{-2} . The agreement of the daytime fluxes is good as well and differences can be attributed to different footprints as the profile measurements are always fixed to the temperature level 0.03 m and on a very small spatial scale, whereas the flux measurements have a footprint size of about 10 m. This might be indicated by the fact that the agreement in timing of the peaks of profile-derived fluxes and eddy covariance fluxes shifts from day to day. Furthermore, fluxes derived from the upper measurement heights that have a larger footprint agree better. The horizontal inhomogeneity of the ground cover (Chap. 2) and the sunflecks might be responsible for the deviations in the afternoon as well, where modelled sensible heat fluxes drop to about zero right after the peak, whereas the eddy fluxes are still positive. Other reasons for this discrepancy in the afternoon might be the well-mixed conditions that cause temperature differences between the heights to be in the uncertainty range of the temperature sensors (0.1 K). Furthermore, in the afternoon the cooling starts first at the forest floor, while the sensible heat flux at 1 m is still positive and larger.

8.3.2.3 Stability

From the wind and temperature profiles, the stability of the air column close to the forest floor can be determined by the bulk Richardson number (Ri_B) and the stability parameter $\zeta = z/L$, with L being the Obukhov length and z the reference height. The calculations have been done for different heights within the profile. Figure 8.2 shows the results for the layers 0.03 m to 0.3 m and from 0.3 m to 0.9 m. The values of both methods generally agree well for ζ derived from local measurements (wind and temperature gradients). The agreement between the different heights is good as well. But in general, the agreement between both methods is better than between the different layers. For some periods, nighttime values of the upper layer exceed the critical Richardson number (0.2), whereas at the lower levels values are close to zero and therefore in better agreement with the eddy covariance measurements. Only for some unstable episodes is the agreement between the upper levels and the eddy covariance derived stability better than for the lower level. Some of the deviations (e.g., timing of unstable conditions) between the values derived from profiles and those from eddy covariance might be caused by different radiation regimes (horizontal separation of systems) as discussed above, as the unstable conditions are clearly linked to heating of the surface by direct sunlight in the sunflecks. Depending on stability, the footprint of the eddy covariance measurement is about 10 m. Therefore, the profile should be within the footprint of the sonic (3 m horizontal separation) most of the time, but the footprint of the profile is much smaller, especially for the lower levels. Nevertheless, at low wind speeds, due to nearby obstacles (stems) and under stable conditions without well-developed turbulence, the eddy covariance measurements are prone to difficulties as well (e.g., for forest floor measurements Baldocchi and Meyers 1991; Subke and Tenhunen 2004; Launiainen et al. 2005). As can already be seen from the temperature profiles, predominantly neutral conditions prevail and unstable and stable episodes occur in the morning and evening, respectively (see Figs. 8.1 and 8.2). Neutral conditions occur mainly from midnight to the early morning and in the afternoon. Eddy covariance measurements show predominately neutral conditions for the whole day with some more randomly distributed stable and unstable episodes. In the morning, unstable conditions occurred simultaneously with the increased radiation, but eddy covariance measurements showed either neutral conditions or shorter stable episodes before and after the values from the local profile. As these episodes are driven by the thermal (static) stability of the air, all three methods applied based on the dynamic stability are not valid during these events. The sunflecks cause local heating of the surface that induces local free convection. In the evening and in the early night, u_* drops to very low values (see Fig. 8.1), and therefore stable stratification develops due to cooling of the surface. These stable episodes coincide with minima in wind speed between 0.3 m and 2 m and changes in wind direction (Fig. 8.1). Another effect that limits the comparability of profile-derived values and eddy covariance measurements is the decoupling of the near forest floor layer. During the decoupling, gradients increase and dynamic stability at 1 m might not be affected.

8.3.3 Comparison of Modelled and Chamber Fluxes

8.3.3.1 Radon Fluxes

The multilayer model was applied to calculate trace gas fluxes as well. As fluxes of ^{222}Rn and CO_2 have been additionally measured at the forest floor by a static chamber, another possibility for intercomparison exists. For the further analysis, only ^{222}Rn was used. Fluxes from the chamber are much lower and less variable. They vary around $0.025 \text{ Bq m}^{-2} \text{ s}^{-1}$, whereas the modelled fluxes are around $0.125 \text{ Bq m}^{-2} \text{ s}^{-1}$ with maxima reaching up to $0.35 \text{ Bq m}^{-2} \text{ s}^{-1}$. Therefore, modelled fluxes are sometimes more than a factor of 10 higher. As radon is a noble gas, it undergoes no chemical reactions and, unlike CO_2 , is not actively taken up by plants. The half-life time (τ) of 3.8 days is sufficiently long to allow radon to be viewed as stable during the closure time of the chamber (50 min; $<1/100\tau$). Therefore, the differences in the flux should be caused by physical processes such as different pressure within and outside the chamber or a different diffusion gradient. As a third independent approach (like eddy covariance) is missing for radon fluxes, deciding which approach failed is not straightforward. The model has been shown to reproduce the sensible heat flux very well (esp. given the difficulties of the inhomogeneous radiation field at the forest floor). The enclosures are known to suffer from different problems that can lead to either overestimation or underestimation of the flux. In our study the flux was calculated by using a linear fit of the concentration rise. Recent publications suggest that linear fits tend to underestimate the flux (e.g., Davidson et al. 2002; Kutzbach et al. 2007). According to Davidson and coworkers (2002), underestimation was in the range of 5–15 %, but due to the higher uncertainty of the nonlinear fit, they preferred a linear fit. Kutzbach et al. (2007) found 70 % underestimation due to the use of linear fits instead of an exponential model. Nevertheless, they report as well that the curvatures often deviate from the theoretical model, pointing to disturbances of the soil flux by the chamber. An overpressure of just 0.5 Pa was reported to reduce the flux by 70 % (Lund et al. 1999). As the chamber flux is fairly constant, the deviation to the modelled flux varies a lot: from 0 % to 85 % lower fluxes. In principle, the chamber design was intended to deal with the above-discussed problems. The chamber had a height of about 20 cm (depending on the depth it was buried into the ground) and was equipped with a capillary as a vent to equilibrate the pressure. Nevertheless, the differential pressure between the chamber and ambient has not been measured and therefore pressure effects cannot be excluded. Furthermore, (wind-induced) pressure differences might even be unmeasurable as they are compensated by mass flows in/out of the soil (Bain et al. 2005), which are the reason for the altered CO_2 flux as well. Also the larger volume (20 cm height) used to avoid fast accumulation was overcome by the comparably long closure time (50 min) that was necessary for measuring radon in parallel (maximum time resolution for one data point is 10 min). The chamber was additionally equipped with a fan to provide complete mixing. The fan destroys the natural gradient above the soil and was thought to

increase the flux by increasing the gradient between the soil air and the chamber air. Nevertheless, it seems that due to the long closure time, the opposite effect dominates: the rising concentration in the chamber reduces the flux. Furthermore, pressure fluctuations have been proposed to be an important driver of mass transport across the soil-air interface (Kimball and Lemon 1971). Depending on the pressure fluctuations induced by the fan, this effect can be larger or lower than in outside air. But even technically advanced systems still suffer from the enclosure technique itself by changing the exchange conditions and the preventing cooling of the surface by outgoing longwave radiation (Riederer et al. 2014). An alternative method of determining near-surface fluxes might be provided by the “thoron clock” (Lehmann et al. 1999; Plake and Trebs 2013), which just needs a measured thoron (^{220}Rn) gradient and no enclosures.

8.3.3.2 Carbon Dioxide Fluxes

Similar results as for ^{222}Rn were obtained for CO_2 . As can be seen in Fig. 8.3, the CO_2 flux determined from the chamber is much less variable and somehow marks a lower limit for the modelled flux. With regard to the mean modelled flux, the chamber flux is lower by about a factor of 2.5. Besides this difference, the modelled and the chamber fluxes are both always positive, which is related to the same ground cover for both measurements (measurements co-located on moss) without substantial assimilation. Therefore, only respiration fluxes were

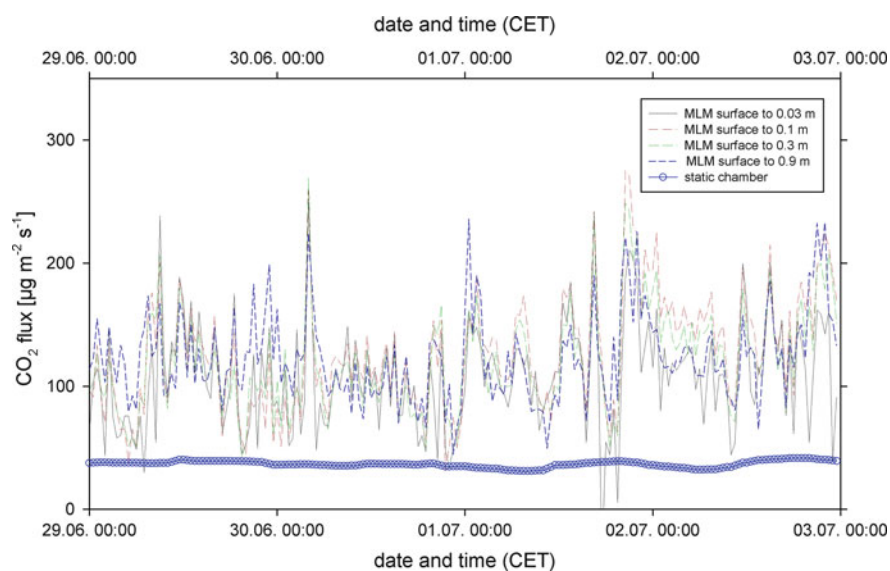


Fig. 8.3 CO_2 fluxes as modelled by the multilayer model (MLM) for different layers compared to those measured by a collocated static chamber system

measured. Unfortunately, no co-located CO₂ eddy covariance measurements were available, but the magnitude and dynamics of the modelled values agree much better with respiration fluxes from the Waldstein site derived from conditional sampling (Thomas et al. 2008) than the chamber fluxes. This therefore supports the argumentation derived for ²²²Rn that the chamber measurements most probably failed to produce reasonable fluxes.

8.3.4 Determination of the Coupling Situation at the Forest Floor

As discussed above, the multilayer model was shown to reproduce sensible heat fluxes very well and has therefore been used to calculate trace gas fluxes from profiles, while static chamber measurements failed to produce reasonable fluxes and were therefore excluded from further analysis. In the case of CO₂, the only available eddy covariance measurements (not shown here) in the trunk space were about 80 m away, over a different ground cover. Therefore, the values were not comparable. The measured (eddy covariance) and modelled O₃ fluxes will be discussed below. Another possibility for comparison, but more importantly for the detection of coupling and decoupling in the lowest meter, was to use the multilayer model for calculation of an effective surface concentration that was compared to measured surface concentrations. The agreement of those two concentrations was then used as a measure of whether the near forest floor layer was coupled or decoupled from the layers above. The RS approach was thereby used to calculate a flux from the profile, and subsequently the multilayer model was used to calculate an effective surface concentration from that flux.

Radon is best suited for this kind of investigation as it does not react or change its phase (as does water) nor is it influenced by plants (fixation, evapotranspiration, etc.). It is therefore not influenced by chemical or physical processes other than transport, at least in a reasonably short time compared to the decay time (3.8 d). As can be seen in Fig. 8.4, periods with large discrepancies (with even peaks in opposite directions) alternate with periods with good agreement between modelled and measured surface concentration. They are marked C_x for coupled situations and D_x for decoupled situations ($x = 1, 2, 3, \dots$). For decoupled situations we can distinguish two different cases with respect to the model. Either the decoupling takes place between 0.1 m and 0.3 m (the profile heights used for modelling) or decoupling occurs below 0.1 m. In the first case, the gradient increases, and the model therefore overestimates the effective surface concentration because the flux given by the RS parameterization is overestimated. In the latter case, the decoupling takes place below the lower profile height used to calculate the flux. The ²²²Rn accumulation below the heights used for the calculation of the effective surface concentration leads to an underestimation. Significantly higher ²²²Rn concentrations were observed at 0.3 m than at 0.03 m for some periods. Therefore, the gradient is

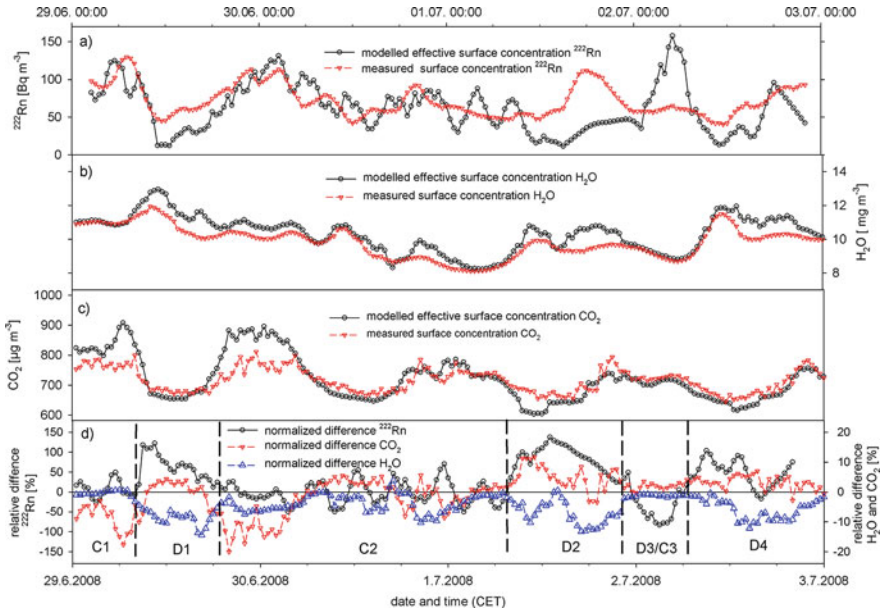


Fig. 8.4 Modelled effective surface concentrations and measured surface concentrations for (a) ^{222}Rn , (b) water vapor, and (c) CO_2 . The ^{222}Rn data have been smoothed by a moving average (window size 5). Frame (d) shows the relative difference (difference normalized to the mean) between measured and modelled values

reversed. This might be due to the advection of ^{222}Rn , as its lifetime is sufficiently long and its emanation from the ground is very heterogeneously distributed. A drawback of the use of ^{222}Rn is its low activity relatively to the sensors' sensitivity and the low time resolution of the measurements. In combination with the heterogeneous distribution of the ^{222}Rn emanation, the signals are very variable, and therefore relative differences between measured and modelled surface concentration reach up to a factor of two. Without smoothing the signal with a moving average (window size 5), the relations between the signals would be hardly visible. Nevertheless, during some periods agreement is comparably good and the periods are therefore labeled as coupled. As the relative error of the ^{222}Rn measurement is 40 %, the relative difference of ± 50 % between measured and modelled surface concentrations is still regarded as good agreement. In principle, coupling derived from water vapor and CO_2 (see below) confirms these periods, although these measurements are associated with other problems as discussed below.

8.3.4.1 Water Vapor

Water vapor does not react in significant amounts in the troposphere and can therefore be regarded as chemically inert as well. Unlike radon, it undergoes phase

changes (condensation/evaporation) and its cycling is altered by vegetation due to transpiration. Also unlike radon, the effective surface concentration tends to be higher than the measured concentration for all situations (Fig. 8.4). The tendency for overestimation of the effective surface concentration for water vapor might be due to the different footprints for the different heights. The surrounding ground cover vegetation is thought to increase water vapor levels in the upper heights of the profile due to transpiration, whereas the very local measurements at 0.03 m are on a much dryer surface. Nevertheless, the covariation of both curves (measured and modelled) is higher than for ^{222}Rn and the relative deviation is much smaller (mostly <10 %). This is probably due to the higher sensitivity of the analyzer compared to the ^{222}Rn measurements. Nevertheless, deviation of the values is largest during decoupled situations as well. Only for the decoupled case (D3) that had opposite peaks in the case of ^{222}Rn does water vapor show an almost perfect agreement between modelled and measured concentration (relative difference <5 %). During this period the site was influenced by a strong low-level jet (not explicitly shown in Chap. 11). But as shown in another example in Chap. 11, the low-level jets can enhance mixing from air layers above the canopy down to the forest floor during nighttime.

8.3.4.2 Carbon Dioxide

Modelled and measured CO_2 concentrations agree generally well (within 10 %). Similar to ^{222}Rn and water vapor, periods with good agreement alternate with those having larger deviations of measured and modelled concentrations. These periods agree, in principle, with those also found for ^{222}Rn and water vapor. Other than for water vapor, which was consistently overestimated, CO_2 shows overestimation during nighttime and slight underestimation during daytime, which is clearly visible from Fig. 8.4 for at least the first 2 days. As already discussed for H_2O , this might be caused by the surrounding vegetation that is within the footprint of the upper heights of the profile. The higher nighttime values are due to additional respiration by the plants and the lower daytime values due to assimilation.

Therefore, all three trace gases show a consistent picture. Periods of good vertical coupling and decoupling alternate, but detection of local coupling/decoupling is hampered by the different footprints of the profile heights and the high variability of forest floor fluxes.

8.3.5 Reactive Trace Gases

The reactive trace gases NO , NO_2 , and O_3 form a so-called triad by forming a set of chemical reactions where NO and O_3 combine to NO_2 and are reformed by photolysis of NO_2 . They form a photo stationary state that can be expressed by the Leighton ration (Leighton 1961). As the photolysis frequency of NO_2 is

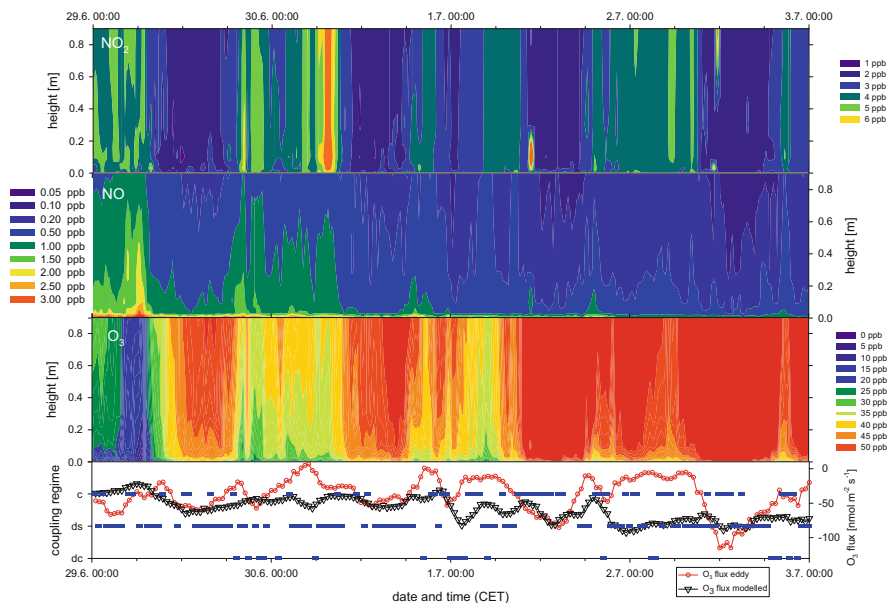


Fig. 8.5 Contour plot of the mixing ratios of the reactive trace gases NO_2 , NO , and O_3 in the lowest meter above ground. For comparison the measured and modelled (from the gradients) O_3 fluxes are shown together with the coupling regimes of the 2 m eddy measurement with the above layers. Dc (decoupled canopy whole canopy decoupled from the air layer above), Ds (decoupled subcanopy only subcanopy decoupled), and C (fully coupled canopy)

comparably low at the forest floor (10% from above canopy) and NO values are comparably high due to the well-known microbial soil emissions, consumption of NO and O_3 and therefore production of NO_2 dominate. This is shown in Fig. 8.5 by the anti-correlation of NO and O_3 values. In addition to the direct chemically induced anti-correlation, during the course of the week NO emissions decline and O_3 formation (above canopy) increases. This is due to the dry conditions after a rain event on the 25th of June. Ozone mixing ratios are well known to increase in warm dry weather (e.g., US-EPA 2006; Bloomer et al. 2010), and NO emissions have been found to peak after rain events (e.g., Davidson 1992; Scholes et al. 1997). As the background of NO_2 is quite variable, the formation of NO_2 is less obvious, but NO_2 values often showed maximum values at around 1 m. Furthermore, higher NO_2 values often coincide with high values of NO and low O_3 values (Fig. 8.5). The NO_2 background is mainly influenced by transport of anthropogenic and biogenic emissions. Although during daytime NO is formed by photolysis of NO_2 above canopy and is transported downward (e.g., Horii et al. 2004; Foken et al. 2012; Chap. 9), clear profiles with largest values at the soil surface were observed for NO , pointing to the dominance of NO soil emissions close to the ground. The accumulation of NO that follows the depletion of O_3 seems to be more related to the decoupling of the trunk space from above air layers (see Fig. 8.5), as steep NO and

O₃ gradients in the first meter are not linked to the decoupling and coupling of the near forest floor layer as determined in the previous section from comparison of the effective surface concentrations of ²²²Rn, H₂O, and CO₂ (see above and Fig. 8.4).

8.3.5.1 Ozone Fluxes

In the case of O₃, nearby eddy covariance measurements (1 m height, see Chap. 9) could be compared to the modelled flux of the multilayer model. Reactive trace gases, such as O₃, entail difficulties for such intercomparison, as due to chemical reactions, they have sources or sinks within the measured profile. Therefore, the flux is not constant with height, which is one of the general assumptions for the application of profile methods. Next to the reactions of O₃ directly at the soil surface or uptake to ground vegetation, the gas phase reaction with (soil emitted) nitrogen oxide (NO) is the main sink at the forest floor. The eddy covariance flux represents the total (deposition and chemical reactions) flux at 1 m height, while the modelled fluxes integrate the profile from the surface or 0.3 m up to 0.9 m. All fluxes are negative as the soil is solely a sink for O₃, and O₃ sources are located above canopy. Both fluxes vary within the same range but the eddy covariance fluxes are predominately lower. The modelled fluxes generally overestimate the flux compared to the eddy covariance measurements predominantly at times when large gradients of O₃ are observed in the lowest meter. The large gradients are presumably caused by the titration of O₃ by NO during times of low mixing (see Fig. 8.5). In such cases, chemical reactions act faster than the transport, causing a so-called chemical flux. A measure for the dominance of transport over chemistry or vice versa is the Damköhler number (Damköhler 1940). Therefore, modelling based on gradient methods overestimates the flux if Damköhler numbers are in the critical range $0.1 < Da < 10$. The periods of good agreement of modelled and measured fluxes are characterized by high O₃ and low NO values (longer chemical timescale). Furthermore, high O₃ values and low gradients are observed down to the lowest measurement level during these periods. It seems, by comparison of the fluxes, that these are more influenced by the coupling of the trunk space to the air layers above (Chaps. 6 and 11) than by decoupling of the surface as discussed above. Regarding the coupling of the canopy by coherent exchange, mixing ratio differences down to 0.9 m were lower during coupled situations (Foken et al. 2012). Effective coupling at least down to 0.5 m from about 10:00 to 13:00 local time was determined for the measurements of nitrous acid (HONO) during IOP 1 (Sörgel et al. 2011; Chap. 1), serving as a hint that decoupling might be related to a small layer very close to the surface during times of a well-coupled canopy. As the ground surface is an irreversible sink for O₃, the O₃ concentration must approach zero at the surface. As O₃ values at the lowest measurement level (0.005 m) are, on average, 26 ppb with a minimum of 4.5 ppb and a maximum of 55 ppb, the gradients in the lowest layer or in the laminar layer must be very steep. Therefore, the canopy coupling just seems to influence the height of the layer in the proximity of the surface, where O₃ depletion is strongest.

8.4 Conclusions

Some of the challenges for flux measurements at the forest floor are the heterogeneity of sources, the presence of local obstacles, the inhomogeneous radiation and the intermittent turbulence with occasionally decoupling of the different layers. Thereby, two different mechanisms of decoupling: (a) the coupling of the forest canopy by coherent structures (see Chaps. 6 and 11) and (b) the decoupling of the near forest floor layer. To identify coupling or decoupling, the magnitude and the sign of fluxes are compared. We successfully tested a new approach to the detection of decoupling of the near forest floor layer by calculating an effective surface concentration from a given flux with a multilayer model and comparing this to measured concentrations. Measured eddy covariance and modelled sensible heat fluxes from the multilayer model showed surprisingly good agreement, which was not expected based on the heterogeneity of available energy at the forest floor and the generally low fluxes (max. 25 W m^{-2}) that were often close to the detection limit of the eddy covariance method. As the multilayer model was shown to reproduce the sensible heat flux very well, it is assumed to be a suitable tool for deriving fluxes of (reactive) trace gases as well. When compared to CO_2 and ^{222}Rn flux measurements obtained by a static chamber system, no good agreement was found. This was probably caused by one of the well-known technical problems of enclosures that can alter the soil flux. Therefore, chamber measurements should always be validated against an independent measurement at the best co-located eddy covariance measurements. But even the best technical solutions will still suffer from the disturbed exchange conditions caused by enclosing the above soil air. Therefore, other methods of inferring soil fluxes should be favored.

Another advantage of using the model was that it allowed the calculation of effective surface concentrations that could be compared to measured surface concentrations for several tracers (including ^{222}Rn , H_2O , CO_2 , and O_3) and subsequently be used to infer the decoupling of the near forest floor layer. Radon is, in principle, perfectly suited for such a task as it is chemically inert and is emitted solely from the ground. It turned out, however, that the precision and time resolution of the ^{222}Rn measurements put limits on this method. Furthermore, ^{222}Rn has a lifetime sufficient for it to be advected, which disturbs the local gradients. In addition, due to heterogeneous sources and sinks at the forest floor, the different footprints of the heights of the profile represent averages of different fluxes, which interfere with the comparison of a very local surface condition. Nevertheless, periods of good agreement of measured and modelled effective surface concentration were similar for ^{222}Rn , H_2O , and CO_2 . The agreements (and disagreement) of modelled and measured surface concentration was used to infer coupling or decoupling of the ground surface from the air layers above. So far, the decoupling of the near forest floor layer has not been reported, although it has important implications on how soil-chamber and in-soil measurements can be linked to measurements in or above the trunk space. As a consequence, respiration fluxes derived from conditional sampling of eddy covariance fluxes above canopy

(Chap. 6) have to be revisited as well. Nevertheless, the gradients of reactive trace gases and also the fluxes of O_3 seemed to be predominantly influenced by the coupling with the above layers by coherent structures and to a lesser extent by the decoupling of the soil layer, but the canopy coupling only influenced the height of the layer where most of O_3 depletion is strongest. Assessment of the influence of the decoupling of the near forest floor layer on the magnitude of trace gas fluxes is not straightforward and needs longer time series of collocated eddy covariance fluxes and highly resolved profiles in the lowest meter above ground. Nevertheless, the results show that profile measurements close to the ground are important for validating the link between fluxes in and out of the soil determined by laboratory or chamber measurements and fluxes measured in the trunk space. As sensible heat fluxes showed good agreement, one might further focus on the temperature by (a) using fiber-optic distributed temperatures sensing (Thomas et al. 2012) which will overcome the problem of measured gradients becoming more local with decreasing height and (b) by using infrared surface temperature sensors or cameras to compare the “real” surface temperature to those modelled from the gradients and fluxes. Furthermore, the use of ^{220}Rn instead of ^{222}Rn will lead to more counts and almost no advection due to the low radioactive decay time (56 s).

Acknowledgment The authors gratefully acknowledge financial support by the German Science Foundation (DFG projects EGER, FO 226/16-1, ME 2100/4-1 and ZE 792/4-1) and by the Max Planck Society. For borrowing a static chamber and two radon monitors, we would like to thank Franz Conen from the Department of Environmental Sciences of the University of Basel. We would like to thank Johannes Lüers and Korbinian Hens for sharing their experience with radon measurements at the Waldstein site.

References

- Bain WG, Hutryra L, Patterson DC, Bright AV, Daube BC, Munger JW, Wofsy SC (2005) Wind-induced error in the measurement of soil respiration using closed dynamic chambers. *Agric For Meteorol* 131:225–232
- Baldocchi DD, Meyers TP (1991) Trace gas exchange above the floor of a deciduous forest: 1. Evaporation and CO_2 efflux. *J Geophys Res* 96(D4):7271–7728
- Bloomer BJ, Vinnikov KY, Dickerson RR (2010) Changes in seasonal and diurnal cycles of ozone and temperature in the eastern U.S. *Atmos Environ* 44:2543–2551
- Damköhler G (1940) Der Einfluss der Turbulenz auf die Flammengeschwindigkeit in Gasmischungen. *Z Elektrochem* 46:601–652
- Davidson EA (1992) Pulses of nitric oxide and nitrous oxide flux following wetting of dry soil: an assessment of probable sources and importance relative to annual fluxes. *Ecol Bull* 42:149–155
- Davidson EA, Savage K, Verchot LV, Navarro R (2002) Minimizing artifacts and biases in chamber-based measurements of soil respiration. *Agric For Meteorol* 113:21–37
- Foken T (1979) Vorschlag eines verbesserten Energieaustauschmodells mit Berücksichtigung der molekularen Grenzschicht der Atmosphäre. *Z Meteorol* 29:32–39
- Foken T (1984) The parametrisation of the energy exchange across the air-sea interface. *Dyn Atmos Oceans* 8:297–305
- Foken T (2008) *Micrometeorology*. Springer, Berlin, Heidelberg, 308 pp, (2nd edition 2017)

- Foken T, Kitajgorodskij SA, Kuznecov OA (1978) On the dynamics of the molecular temperature boundary layer above the sea. *Bound-Lay Meteorol* 15:289–300
- Foken T, Meixner FX, Falge E, Zetzsch C, Serafimovich A, Bargsten A, Behrendt T, Biermann T, Breuninger C, Dix S, Gerken T, Hunner M, Lehmann-Pape L, Hens K, Jocher G, Kesselmeier J, Lüers J, Mayer JC, Moravek A, Plake D, Riederer M, Rütz F, Scheibe M, Siebicke L, Sörgel M, Staudt K, Trebs I, Tsokankunku A, Welling M, Wolff V, Zhu Z (2012) Coupling processes and exchange of energy and reactive and non-reactive trace gases at a forest site—results of the EGER experiment. *Atmos Chem Phys* 12:1923–1950
- Horii CP, Munger JW, Wofsy S, Zahniser M, Nelson D, McManus JB (2004) Fluxes of nitrogen oxides over a temperate deciduous forest. *J Geophys Res* 109:D08305
- Hübner J, Siebicke L, Lüers J, Foken T (2016) Forest climate in vertical and horizontal scales. In: Foken T (ed) *Energy and Matter Fluxes of a Spruce Forest Ecosystem*. Springer, Berlin, Heidelberg
- Kimball BA, Lemon ER (1971) Air turbulence effects upon soil gas exchange. *Soil Sci Soc Am J* 35:16–21
- Kutzbach L, Schneider J, Sachs T, Giebels M, Nykänen H, Shurpali NJ, Martikainen PJ, Alm J, Wilkening M (2007) CO₂ flux determination by closed-chamber methods can be seriously biased by inappropriate application of linear regression. *Biogosciences* 4:1005–1025
- Launiainen S, Rinne J, Pumpanen J, Kulmala L, Kolari P, Keronen P, Siivola E, Pohja T, Hari P, Vesala T (2005) Eddy covariance measurements of CO₂ and sensible and latent heat fluxes during a full year in a boreal pine forest trunk-space. *Boreal Environ Res* 10:569–588
- Lehmann BE, Lehmann M, Neftel A, Gut A, Tarakanov SV (1999) 220 Radon calibration of near-surface turbulent gas transport. *Geophys Res Lett* 5:607–610
- Lehmann BE, Neftel A, Tarakanov SV (2001) Continuous on-line calibration of diffusive soil-atmosphere trace gas transport using vertical ²²⁰Rn- and ²²²Rn activity profiles. *Radiochim Acta* 11–12:839–843
- Lehmann BE, Ihlya B, Salzmann S, Conen F, Simon E (2004) An automatic static chamber for continuous ²²⁰Rn and ²²²Rn flux measurements from soil. *Radiat Meas* 38:43–50
- Leighton PA (1961) *Photochemistry of air pollution*. Academic Press, New York
- Lüers J, Bareiss J (2010) The effect of misleading surface temperature estimations on the sensible heat fluxes at a high Arctic site—the Arctic Turbulence Experiment 2006 on Svalbard (ARCTEX-2006). *Atmos Chem Phys* 10:157–168
- Lund CP, Riley WJ, Pierce LL, Field B (1999) The effects of chamber pressurization on soil-surface CO₂ flux and the implications for NEE measurements under elevated CO₂. *Glob Chang Biol* 5:269–281
- Misson L, Baldocchi DD, Black TA, Blanken PD, Brunet Y, Curiel Yuste J, Dorsey JR, Falk M, Granier A, Irvine MR, Jarosz N, Lamaud E, Launiainen S, Law BE, Longdoz B, Loustau D, McKay M, Paw U KT, Vesala T, Vickers D, Wilson KB, Goldstein AH (2007) Partitioning forest carbon fluxes with overstory and understory eddy-covariance measurements: a synthesis based on FLUXNET data. *Agric For Meteorol* 144:14–31
- Nordbo A, Järvi L, Vesala T (2012) Revised eddy covariance flux calculation methodologies—effect on urban energy balance. *Tellus Ser B* 64:18184. doi:10.3402/tellusb.v64i0.18184
- Plake D, Trebs I (2013) An automated system for selective and continuous measurements of vertical thoron profiles for the determination of transport times near the ground. *Atmos Meas Tech* 6:1017–1030
- Richter SH, Skeib G (1984) Anwendung eines Verfahrens zur Parametrisierung des turbulenten Energieaustausches in der atmosphärischen Bodenschicht. *Geod Geophys Veröff*, R II 26:80–85
- Richter SH, Skeib G (1991) Ein Verfahren zur Parametrisierung von Austauschprozessen in der bodennahen Luftschicht. *Abh Meteorol Dienstes DDR* 146:15–22
- Riederer M, Serafimovich A, Foken T (2014) Eddy covariance—chamber flux differences and its dependence on atmospheric conditions. *Atmos Meas Tech* 7:1057–1064

- Scholes MC, Martin R, Scholes RJ, Parsons D, Winstead E (1997) NO and N₂O emissions from savanna soils following the first simulated rains of the season. *Nutr Cycl Agroecosyst* 48:115–122
- Serafimovich A, Thomas C, Foken T (2011) Vertical and horizontal transport of energy and matter by coherent motions in a tall spruce canopy. *Bound-Lay Meteorol* 140:429–451
- Skeib G (1980) Zur Definition universeller Funktionen für die Gradienten von Windgeschwindigkeit und Temperatur in der bodennahen Luftschicht. *Z Meteorol* 30:23–32
- Sodemann H, Foken T (2005) Special characteristics of the temperature structure near the surface. *Theor Appl Climatol* 80:81–89
- Sörgel M, Trebs I, Serafimovich A, Moravek A, Held A, Zetzsch C (2011) Simultaneous HONO measurements in and above a forest canopy: influence of turbulent exchange on mixing ratio differences. *Atmos Chem Phys* 11:841–855
- Subke JA, Tenhunen JD (2004) Direct measurements of CO₂ flux below a spruce forest canopy. *Agric For Meteorol* 126:157–168
- Thomas C, Foken T (2007) Flux contribution of coherent structures and its implications for the exchange of energy and matter in a tall spruce canopy. *Bound-Lay Meteorol* 123:317–337
- Thomas C, Martin J, Goeckede M, Siqueira M, Foken T, Law B, Loescher H, Katul G (2008) Estimating daytime subcanopy respiration from conditional sampling methods applied to multi-scalar high frequency turbulence time series. *Agric For Meteorol* 148:1210–1229
- Thomas CK, Kennedy AM, Selker JS et al (2012) High-resolution fibre-optic temperature sensing: a new tool to study the two-dimensional structure of atmospheric surface layer flow. *Bound-Lay Meteorol* 142:177–192. doi:[10.1007/s10546-011-9672-7](https://doi.org/10.1007/s10546-011-9672-7)
- U.S. EPA (2006) Air quality criteria for ozone and related photochemical oxidants. EPA/600/R-05/004aF-cF. U.S. Environmental Protection Agency, Washington, DC
- Zeeman MJ, Eugster W, Thomas CK (2013) Concurrency of coherent structures and conditionally sampled daytime sub-canopy respiration. *Bound-Lay Meteorol* 146:1–15